Coulomb-modified Glauber model description of heavy-ion reaction cross sections

S. K. Charagi
Reactor Analysis and Systems Division, Bhabha Atomic Research Centre, Bombay 400 085, India

S. K. Gupta
Nuclear Physics Division, Bhabha Atomic Research Centre, Bombay 400 085, India
(Received 25 August 1989)

A simple closed-form analytic expression for the heavy-ion reaction cross section, involving nuclear densities of colliding ions and the nucleon-nucleon cross section, has been obtained within the framework of the Glauber model modified for the Coulomb field effect. Reaction cross sections for a large number of heavy-ion systems have been predicted reasonably well over an energy range beginning with the Coulomb barrier to a few GeV/nucleon.

I. INTRODUCTION

One of the most fundamental quantities characterizing nuclear reactions is the total reaction cross section σ_R that has been studied extensively for heavy ions both theoretically[1-7] and experimentally.[7-18] The reaction cross sections also find application[19] in diverse research areas such as radiobiology and space sciences. There are two kinds of theoretical formulations of σ_R that are basically different. The low-energy theory is based on the one-dimensional interaction potential between two spherical nuclei such as the Bass model.[2] In such models the required interaction radius is obtained by parametrizing it as a function of masses of the interacting nuclei and by fitting the experimental data. There is no first-principle prediction of the interaction radius, and such models cannot be extrapolated much beyond the data set with which they are fitted. They are unable to describe the reaction cross section beyond 10–15 MeV/nucleon above the Coulomb barrier. The second kind of theory is the high-energy microscopic Glauber theory based on the individual nucleon-nucleon collisions in the overlap volume of the colliding nuclei. We modify this theory to take into account the Coulomb effect. Under certain reasonable approximations a closed expression for the reaction cross section has been derived. We find that this expression describes quite well the reaction cross section over a wide energy range, right from a few MeV/nucleon to a few GeV/nucleon for several systems of colliding nuclei.

II. THE MODEL

To begin with we describe the formulation for σ_R in the absence of the Coulomb field, which will be discussed subsequently. In the absence of the Coulomb field for a finite-range interaction the nucleus-nucleus reaction cross section in the framework of Glauber model can be written as

$$\sigma_R(\text{mb})=20\pi\int b\,db\left[1-\exp\left[-\frac{\bar{\sigma}_{NN}}{10}\int d^2b_1\int d^2b_2 f(|\mathbf{b}_1-\mathbf{b}_2|)\rho_z^1(\mathbf{b}_1)\rho_z^2(|\mathbf{b}_2-\mathbf{b}|)\right]\right], \tag{1}$$

where $\bar{\sigma}_{NN}$ is the nucleon-nucleon reaction cross section (mb) suitably averaged over the interacting *n-n*, *p-p*, and *n-p* pairs, $\mathbf{b}$ is the impact parameter in fm, and the range function $f(|\mathbf{b}_1-\mathbf{b}_2|)$ is normalized as $\int f(b)d^2b=1$. The thickness function ρ_z^1 and ρ_z^2 are defined later. This expression is derived by neglecting the transverse motion of the nuclei when they pass each other. For the zero-range nuclear interaction Eq. (1) reduces to

$$\sigma_R=20\pi\int b\,db\left[1-\exp\left[-\frac{\bar{\sigma}_{NN}}{10}\int d^2b_1\rho_z^1(\mathbf{b}_1)\rho_z^2(|\mathbf{b}_1-\mathbf{b}|)\right]\right]. \tag{2}$$

The transparency function $T(b)$, i.e., the probability that at impact parameter b, the projectile will pass through the target without interacting is given by

$$T(b)=\exp[-\chi(b)]$$

where

$$\chi(b)=\frac{\bar{\sigma}_{NN}}{10}\int_{-\infty}^{+\infty}d^2b_1\int_{-\infty}^{+\infty}d^2b_2 f(|\mathbf{b}_1-\mathbf{b}_2|)\rho_z^1(\mathbf{b}_1)\rho_z^2(|\mathbf{b}_2-\mathbf{b}|). \tag{3}$$

The thickness function $\rho_z^i(\mathbf{b})$ is given by

$$\rho_z^i(\mathbf{b})=\int_{-\infty}^{+\infty}dz\rho_i((b^2+z^2)^{1/2}) \quad (i=1,2) \tag{4}$$

where ρ_i is the nuclear density.

We can reduce Eq. (1) to a simple closed form analytic expression by assuming a Gaussian density distribution of the form[1]

$$\rho_i(b)=\rho_i(0)\exp(-b^2/a_i^2) . \tag{5}$$

Parameters $\rho_i(0)$ and a_i are adjusted to reproduce the experimentally determined nuclear surface texture, as most of the contribution to the reaction cross section comes from the surface region.

Under the assumption of Gaussian density distribution we can write $\rho_z^1(\mathbf{b}_1)$ and $\rho_z^2(|\mathbf{b}_2-\mathbf{b}|)$ as

$$\rho_z^1(\mathbf{b}_1)=\sqrt{\pi}a_1\rho_1(0)\exp(-b_1^2/a_1^2) , \tag{6}$$

$$\rho_z^2(|\mathbf{b}_2-\mathbf{b}|)=\sqrt{\pi}a_2\rho_2(0)\exp[-(b_2-b)^2/a_2^2] . \tag{7}$$

For a finite range nuclear interaction of the form

$$f(b)=\exp(-b^2/r_0^2)/\pi r_0^2 ,$$

where r_0 is the range parameter, $\chi(b)$ can be written as

$$\chi(b)=\frac{a_1a_2\bar{\sigma}_{NN}\rho_1(0)\rho_2(0)}{10r_0^2}\int d^2b_1\int d^2b_2\exp\left[-\frac{(\mathbf{b}_1-\mathbf{b}_2)^2}{r_0^2}\right]\exp\left[-\frac{b_1^2}{a_1^2}\right]\exp\left[\frac{-(\mathbf{b}_2-\mathbf{b})^2}{a_2^2}\right] , \tag{8}$$

Using the identity

$$\int_{-\infty}^{+\infty}e^{-p^2z^2+qz}dz=(\pi^{1/2}/p)\exp(q^2/4p^2) , \tag{9}$$

we can simplify Eq. (8) as

$$\chi(b)=\chi_0\exp[-b^2/(a_1^2+a_2^2+r_0^2)] , \tag{10}$$

where

$$\chi_0=\frac{\pi^2\bar{\sigma}_{NN}\rho_1(0)\rho_2(0)a_1^3a_2^3}{10(a_1^2+a_2^2+r_0^2)} . \tag{11}$$

By substituting Eq. (10) into Eq. (1) we obtain

$$\sigma_R=10\pi(a_1^2+a_2^2+r_0^2)\int_0^{\chi_0}\frac{1-\exp(-\chi)}{\chi}d\chi , \tag{12}$$

and using the identity

$$\int_0^{\chi_0}\frac{1-\exp(-\chi)}{\chi}d\chi=E_1(\chi_0)+\ln\chi_0+\gamma , \tag{13}$$

where γ (Eulers constant)$=0.5772$ and

$$E_1(\chi_0)=\int_{\chi_0}^{\infty}\exp(-\chi)/\chi d\chi ,$$

we obtain the final expression for the total reaction cross section in the absence of the Coulomb field (the Sommerfeld parameter $\eta=0.0$) as

$$\sigma_R(\eta=0)=10\pi(a_1^2+a_2^2+\gamma_0^2)[E_1(\chi_0)+\ln\chi_0+\gamma] , \tag{14}$$

where a_1, a_2, and r_0 are in fm. $E_1(\chi_0)$ is of negligible magnitude as compared to the other two terms in Eq. (14). We will be omitting it in our further discussions.

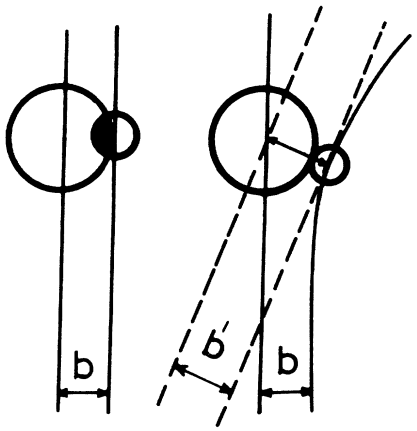

FIG. 1. Schematic of the projectile trajectory with and without Coulomb field.

TABLE I. Comparison of the analytic and the numerical computation of the reaction cross section in *mb* for two $^{40}Ar+^{208}Pb$ and $^{13}C+^{208}Pb$ systems assuming $r_0=0.0$ fm.

System	Energy/nucleon	Reaction cross section in mb	
$^{40}Ar+^{208}Pb$	MeV	Analytic expression (21)	Numerical integration of expression (19)
	6	1457	1503
	10	3121	3150
	14	3755	3776
	18	4064	4081
	22	4234	4248
	26	4337	4346
	30	4394	4405
	34	4431	4440
	38	4452	4460
	44	4465	4472
$^{13}C+^{208}Pb$			
	6	905	945
	10	2219	2224
	14	2715	2733
	18	2955	2970
	22	3086	3098
	26	3161	3171
	30	3205	3214

The expression (14) agrees with that of Karol[1] for the zero range interaction.

The radial distance where $T(b)=0.5$, is called the strong absorption radius R_{int}. Thus

$$R_{\text{int}}^2=(a_1^2+a_2^2+r_0^2)(\ln\chi_0+0.3665)\ , \tag{15}$$

where the value of ln(ln2) has been explicitly put in. The geometrical cross section obtained using Eq. (15) is given by

$$\sigma_R^{\text{Geom}}(\eta=0)=10\pi R_{\text{int}}^2$$
$$=10\pi(a_1^2+a_2^2+r_0^2)(\ln\chi_0+0.3665)\ . \tag{16}$$

The expressions (14) and (16) differ slightly in the last term of the square bracket and yield values agreeing with each other within 3 percent as $\ln(\chi_0)$ is the dominant term. This agreement demonstrates that most of the contribution to σ_R comes from values of b around R_{int} in the $\eta=0$ case.

The expression (14) does not account for the deviation in the eikonal trajectory because of the Coulomb field. In Fig. 1, is shown the deviation in the trajectory because of the Coulomb field. We incorporate this deviation schematically[4] by evaluating the transparency function T at the distance of closest approach b' given by

$$kb'=\eta+(\eta^2+k^2b^2)^{1/2}\ , \tag{17}$$

where k is the wave number and the Sommerfeld parameter

$$\eta=Z_pZ_Te^2/\hbar v\ . \tag{18}$$

Then σ_R is given by

$$\sigma_R=20\pi\int_0^\infty b\,db[1-T(b')]\ . \tag{19}$$

For generalizing Eq. (19) to $\eta\neq0$, case, we can recast the

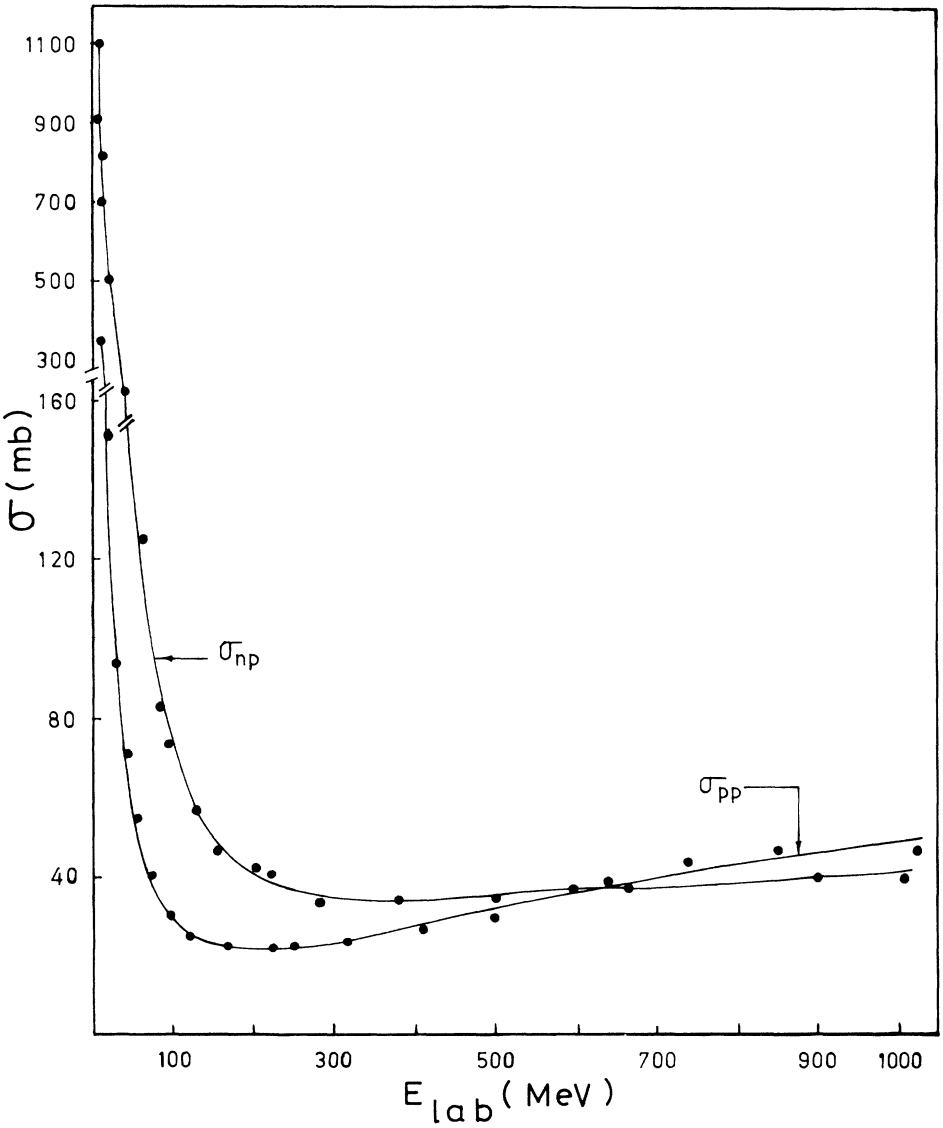

FIG. 2. Plot of a least-squares fit to the nucleon-nucleon cross section data described by Eqs. (22) and (23). The data points (solid circles) are from Ref. 21.

relation (17) as

$$b'^2 = b^2/(1-2\eta/kb') = b^2/[1-V_c(b')/E] , \quad (20)$$

where

$$V_C(b')(\text{in MeV}) = Z_p Z_T e^2/b' = 1.44 Z_p Z_T/b'$$

is the Coulomb potential at b' and E (MeV) is the center-of-mass energy. As most of the contribution to the integral in (19) is from $b' = R_{\text{int}}$, we evaluate it by replacing $V_c(b')$ by $V_c(R_{\text{int}})$ obtaining the analytical expression

$$\sigma_R = 10\pi[1-V_c(R_{\text{int}})/E](a_1^2+a_2^2+r_0^2) \times [E_1(\chi_0)+\ln\chi_0+\gamma] . \quad (21)$$

The accuracy of the approximate expression (21) has been checked by numerically computing the integral (19) along with the definition of b' given by (17). There is an agreement within a few percent between the two that is demonstrated in Table I by the results for two heavy-ion systems ^{40}Ar+^{208}Pb and ^{13}C+^{208}Pb. These calculations were done assuming the zero range nuclear interaction, i.e., the value chosen for $r_0 = 0.0$ fm.

Expression (21) is a simple analytic expression taking into account the effect of the Coulomb field and involves the parameters of the surface normalized nuclear density for both the projectile and the target. In this expression an effective energy or a relative velocity between the colliding nucleons for evaluating $\bar{\sigma}_{\text{NN}}$ is required. The free N-N cross section would be modified by the Fermi motion of nucleons within the nucleus and the Pauli reduction in the phase space. The local relative velocity would also change because of the Coulomb repulsion and the nuclear attraction. Some of these effects may cancel each other and therefore we have made a simple assumption about the relative velocity, taking it to be equal to the asymp-

TABLE II. Gaussian density distribution parameters calculated in the present study by matching the Gaussian density distribution profile function to the two parameter Fermi distribution profile function.

Element	Mass number	rms radius (Ref. 27) (fm)	a_t (fm)	$\rho_t(0)$ (fm^{-3})
Li	6	2.505	1.919	0.160
Be	9	2.512	1.925	0.238
C	12	2.442	1.863	0.354
C	13	2.408	1.829	0.408
O	16	2.710	2.071	0.349
Ne	20	3.010	2.245	0.376
Mg	24	3.015	2.247	0.451
Al	27	3.018	2.249	0.507
Si	28	3.096	2.288	0.515
S	32	3.251	2.362	0.573
Cl[a]	35	3.313	2.390	0.624
Ar	40	3.421	2.437	0.710
Ca	40	3.481	2.463	0.710
V	51	3.610	2.516	0.911
Fe	54	3.700	2.550	0.973
Fe	57	3.760	2.570	1.033
Co	59	3.796	2.588	1.077
Ni	58	3.770	2.578	1.055
Ni	62	3.835	2.603	1.139
Cu	65	3.914	2.632	1.211
Zn	64	3.935	2.640	1.197
Zn	66	3.965	2.650	1.242
Zn	68	3.970	2.653	1.281
Kr[a]	84	4.208	2.737	1.675
Y	89	4.245	2.750	1.793
Zr	90	4.266	2.756	1.824
Nb	93	4.317	2.774	1.913
Ag	107	4.542	2.840	2.366
Sn	118	4.648	2.880	2.709
Xe	136	4.800	2.930	3.306
La	139	4.861	2.947	3.461
Sm	144	4.976	2.982	3.758
Sm	150	5.055	3.006	4.047
Ta	181	5.500	3.134	5.989
Pb	208	5.502	3.134	6.889
Bi	209	5.518	3.319	6.976
U	235	5.811	3.219	9.090
U	238	5.843	3.227	9.362

[a]Calculated using expression (31).

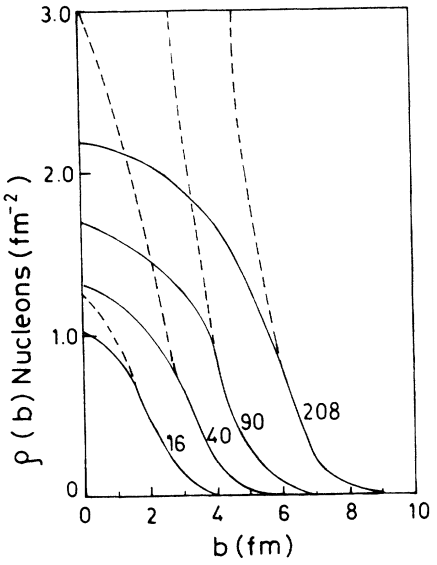

FIG. 3. Variation of profile function with impact parameter for different nuclei of mass 16, 40, 90, and 208. The solid lines are plots for two parameter Fermi density distribution and the dashed lines are the plots for Gaussian density distribution.

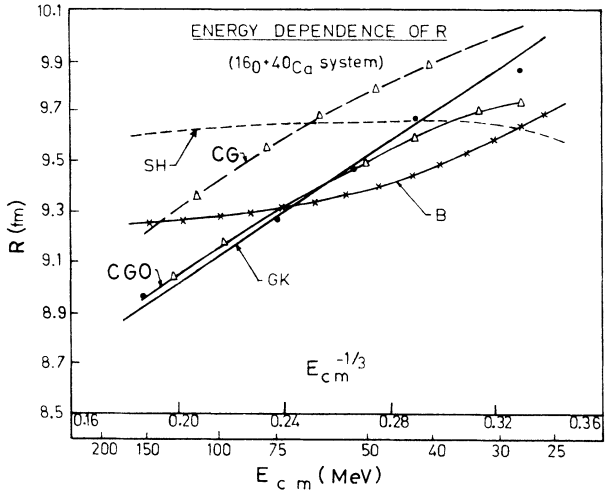

FIG. 5. Energy variation of the interaction radius R_{int} for heavy-ion systems $^{16}O+^{40}Ca$. Solid circles denote experimental values (Ref. 3). GK is based on the model of Gupta and Kailas (Ref. 3). SH is based on the model of Schröder and Huizenga (Ref. 24) and B is based on the model of Bass (Ref. 2). Present work is marked as CG with $r_0=0.92$ fm and CGO with $r_0=0.0$ fm.

totic velocity of the colliding ions for the evaluation of $\bar{\sigma}_{NN}$ that is taken from the nucleon-nucleon scattering.

III. PARAMETRIZATION OF $\bar{\sigma}_{NN}$

Experimentally determined individual nucleon-nucleon cross sections taken from Giacomelli[21] were fitted to the following expressions:[22]

$$\sigma_{np}=-70.67-18.18/\beta+25.26/\beta^2+113.85\beta\ , \tag{22}$$

$$\sigma_{pp}=\sigma_{nn}=13.73-15.04/\beta+8.76/\beta^2+68.67\beta^4\ , \tag{23}$$

where σ_{np} and σ_{nn} are expressed in mb and $\beta=v/c$.

Coefficients in (22) and (23), were obtained by a least-squares fit to the experimental nucleon-nucleon cross section data over a wide energy range right from 10 MeV to 1 GeV. In Fig. 2 these expressions are plotted as solid curves, whereas the solid circles are the data points from Ref. 21. The expression (23) is also used at lower energies. However, at energies lower than 10 MeV we have used for σ_{np} the following expression given by Enge[23]

$$\sigma_{np}=\frac{2.73}{(1-0.0553E_n)^2+0.35E_n}+\frac{17.63}{(1+0.344E_n)^2+6.8E_n}\ , \tag{24}$$

where laboratory energy MeV/nucleon $E_n=\frac{1}{2}*938*\beta^2$. The nucleon-nucleon cross section $\bar{\sigma}_{NN}$ averaged over neutron and proton numbers is calculated by the expression

$$\bar{\sigma}_{NN}(E)=\frac{N_pN_T\sigma_{nn}+Z_pZ_T\sigma_{pp}+N_pZ_T\sigma_{np}+N_TZ_p\sigma_{np}}{A_pA_T}\ , \tag{25}$$

where A_p, A_T, Z_p, Z_T and N_p, N_T are the projectile and the target mass, charge, and neutron numbers, respectively.

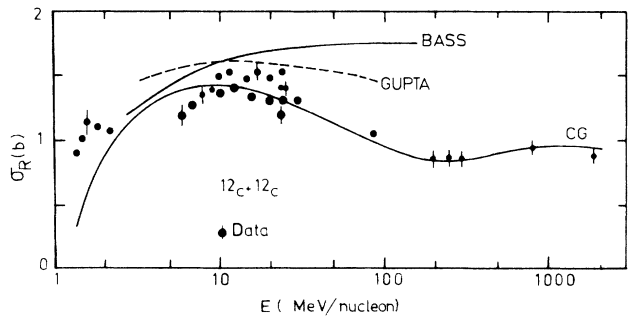

FIG. 4. Total reaction cross section for $^{12}C+^{12}C$ as a function of incident energy. The data points are from the compilation of Ref. 7. The solid and dashed curves are the results of parametrization of Bass (Ref. 2) and of Gupta and Kailas (Ref. 3), respectively. The present calculations are labeled as CG.

IV. CALCULATION OF DENSITY PARAMETERS

The preceding expression (21) has been derived assuming the proton and neutron densities have similar shapes, which seem to be a reasonable approximation. We have derived the nuclear density from the charge density measured by electron scattering by correcting for the charge distribution of protons. Karol[1] has obtained the Gaussian density parameters by fitting the realistic densities in the surface. As the thickness function enters the integral in Eq. (1), we have computed this function and matched it to a Gaussian instead of Karol's prescription. We find

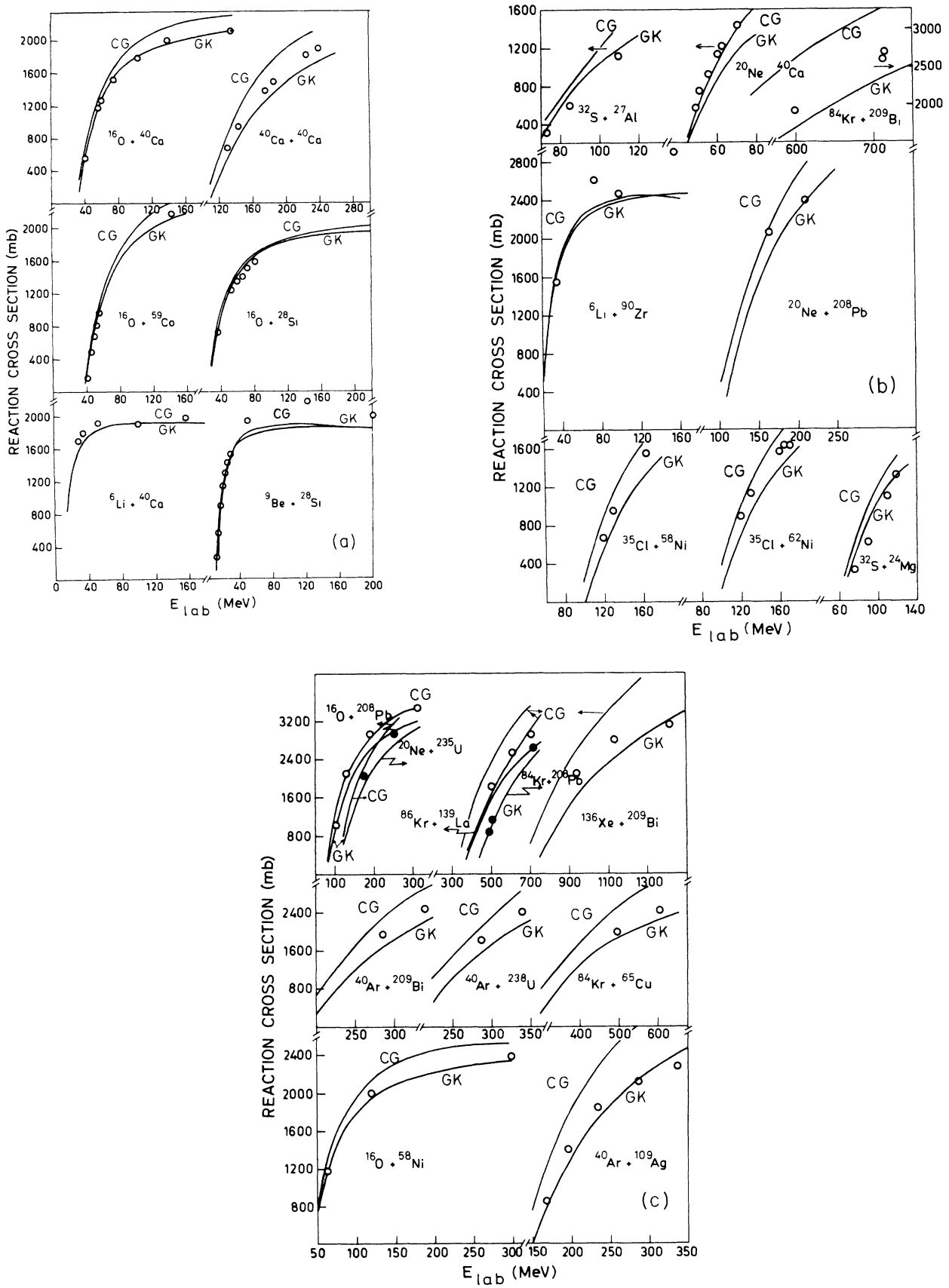

FIG. 6. Comparison of reaction cross section obtained from analyses of elastic scattering data given in Ref. 3 with the predictions from the expression proposed in present work (CG). For comparison the results due to Gupta and Kailas (Ref. 3) labeled as GK are also shown.

this procedure to be more accurate. The parameters $\rho_i(0)$ and a_i are adjusted to reproduce the experimentally determined nuclear surface texture by requiring the function $\rho_z^i(b)$ at $b=c_i$ and $b=c_i+4*d$ in the Gaussian distribution to be identical to the values calculated from the realistic two parameter Fermi distribution, with c_i as the half central density radius and d as the diffuseness parameter.

The two parameter Fermi thickness function (profile function) is given as

$$\rho_{2PF}^i(b)=\int_{-\infty}^{+\infty} dz\, \rho_{0i}/(1+\exp\{[(b^2+z^2)^{1/2}-c_i]/d\}) , \tag{26}$$

where

$$\rho_{0i}=\frac{3A_i}{4\pi c_i^3}\left[1+\frac{\pi^2 c_i^2}{d^2}\right]^{-1} ,$$

which is computed numerically for each individual nucleus at $b=c_i$ and $b=c_i'=c_i+4*d$. These values are matched to the Gaussian distribution profile function of the form

$$\rho_z^i(b)=\bar{K}_i\exp(-b^2/a_i^2) , \tag{27}$$

where

$$\bar{K}_i=\sqrt{\pi}a_i\rho_i(0) .$$

Then a_i can be written as

$$a_i=\{(c_i^2-c_i'^2)/\ln[\rho_{2pF}^i(c_i)/\rho_{2pF}^i(c_i')]\}^{1/2} \tag{28}$$

and

$$\bar{K}_i=\rho_{2pF}^i(c_i)\exp(c_i^2/a_i^2) . \tag{29}$$

The half-central-density radius c_i from rms matter radius is calculated assuming $d=0.53$ fm and using the expression

$$c_i=(5R_{i\,\mathrm{rms}}^2/3-5r_p^2/3-7\pi^2d^2/3)^{1/2} , \tag{30}$$

r_p is the proton charge radius. The data of rms charge radius are taken from the compilation of Angeli and Csatlos.[27]

Table II lists the rms charge radii and a_i and $\mathcal{T}_i(0)$ of various nuclei obtained by the profile function matching technique. For the two nuclei, i.e., ^{35}Cl and ^{84}Kr, where the data of rms charge radius were not available, we have calculated it using the following global expression of Friedrich and Voegler.[20]

$$R_{\mathrm{rms}}=0.891A_i^{1/3}(1+1.565A_i^{-2/3}-1.04A_i^{-4/3}) \tag{31}$$

In Fig. 3 we give the plot of the profile functions. The solid lines depict the results for the two parameter Fermi distribution and broken lines are the Gaussian fits. The agreement between the profiles for the realistic density and the fitted one in surface region is excellent.

V. CALCULATIONS AND RESULTS

In this model there are no free parameters. The range parameter is chosen to be 0.92 fm, which is similar in magnitude to the values given in Ref. 28.

We have studied the variation of $^{12}C+^{12}C$ reaction cross section over a wide energy range. In Fig. 4 we compare the present Coulomb-Glauber calculations labeled as CG with the earlier calculations of Bass[2] and of Gupta and Kailas.[3] The data points in this figure are compiled from various experiments by Kox *et al.*[7] As already mentioned in the Introduction the strong absorption models fail to reproduce the variation of the reaction cross section over the complete energy range. However, the present calculation based on a microscopic approach is in agreement with the experimentally observed variation of the reaction cross section with energy for $^{12}C+^{12}C$.

The present model was also applied to the $^{16}O+^{40}Ca$ systems to calculate the energy variation of interaction radius R_{int}. Figure 5 gives the plot of this variation. In this figure the solid line labeled as GK represents the parametric fit of Gupta and Kailas.[3] For comparison we have plotted results (B) based on the model of Bass[2] and (SH) based on that of Schröder *et al.*[24] The present calculations labeled CG give the values of the interaction radius (R_{int}) higher than the experimental values (solid circles) deduced in Ref. 3 using the data given in Refs. 25 and 26. By setting $r_0=0.0$ fm we get excellent agreement with the calculations. These results are marked as CGO in the figure.

In the low-energy domain we have studied a large number of heavy-ion systems with ^{6}Li to ^{136}Xe as projec-

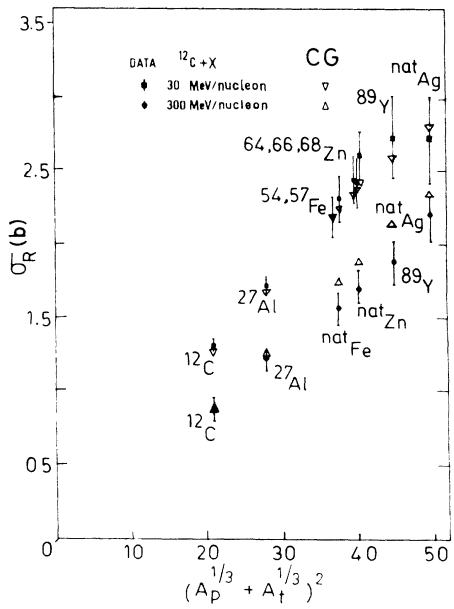

FIG. 7. Measured total reaction cross section for ^{12}C at 30 and 300 MeV/nucleon due to Kox (Ref. 7) are shown as solid circles and squares. Predictions of the present microscopic model are shown as open triangles.

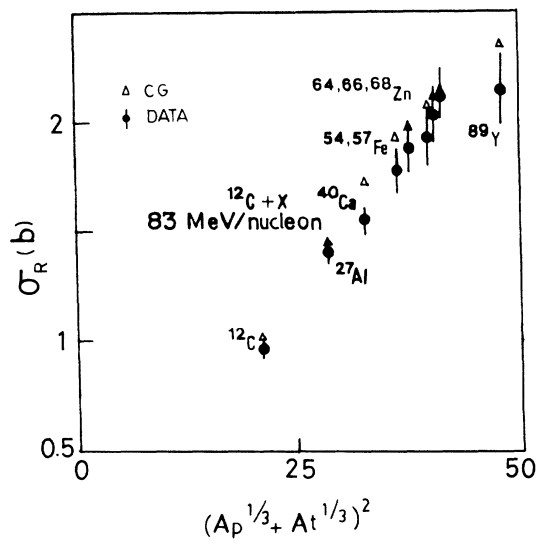

FIG. 8. Same as Fig. 7, but for ^{12}C of 83 MeV/nucleon. The data are from Ref. 7.

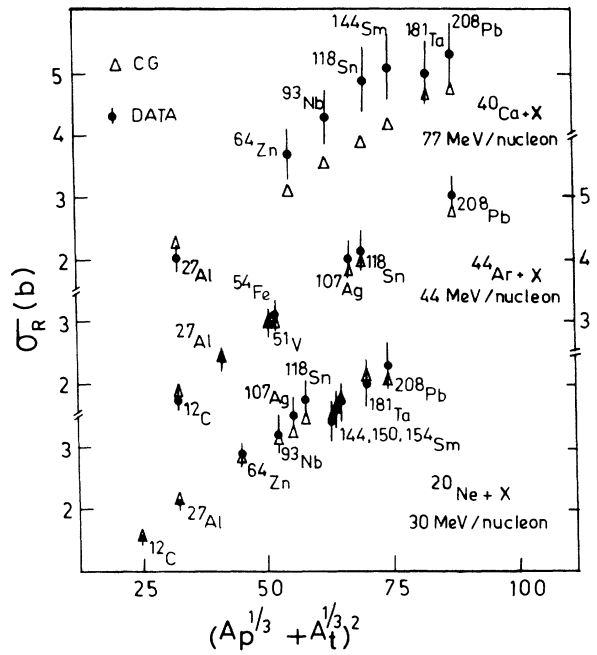

FIG. 9. Total reaction cross section for 30 MeV/nucleon Ne, 44 MeV/nucleon Ar, and 77 MeV/nucleon Ca induced reactions as a function of $(A_p^{1/3}+A_t^{1/3})^2$ compared with the predictions of the present model shown as triangles. The experimental data have been taken from Ref. 13.

tiles and ^{12}C to ^{235}U as targets. For these systems the energy variation of the reaction cross section predicted by the present model is plotted in Figs. 6(a)-6(c) (labeled as CG). For comparison we have also plotted the calculated values (GK) of the reaction cross section based on one parameter model.[3] In most of the cases we have been able to reproduce the data using the simple analytic expression (21).

Kox *et al.*[7] have measured the total reaction cross section of projectile ^{12}C with different targets at 30 and 300 MeV/nucleon. We have calculated reaction cross section for these projectile target systems. The plot of σ_R has been given in Fig. 7 as a function of $(A_p^{1/3}+A_t^{1/3})^2$. Different targets are marked in the figure. Filled circles and squares represent the data due to Kox *et al.* and open triangles depict the present calculations. In most of the cases there is an agreement with the experimental data. We have also compared our calculations with the data of Kox *et al.*[7] at 83 MeV/nucleon for ^{12}C projectile and different targets as shown in Fig. 8.

Brauandet *et al.*[13] have measured reaction cross-section data for 77 MeV/nucleon Ca, 44 MeV/nucleon Ar, and 30 MeV/nucleon Ne. Targets right from the low mass nuclei like ^{12}C to high mass nuclei like ^{208}Pb have been used by them in this measurement. We have compared this data with our calculations as shown in Fig. 9. Except for underprediction of σ_R in case of Ca at 77 MeV/nucleon in general our calculations agree satisfactorily with the data.

VI. CONCLUSIONS

We conclude that the present model, based on a microscopic approach and taking into account the effects of Coulomb field, describes the reaction cross section data reasonably well over a wide energy range. The novel feature of the present model is a simple closed form analytical expression for the reaction cross section, requiring only the nucleon-nucleon cross section and the interacting nuclei densities as input. However, there is a scope for the refinement of the model by incorporating variation of $\bar{\sigma}_{NN}$ with impact parameter. The effect of Fermi motion of nucleons within the nuclei, the real part of optical potential, and modification due to Pauli blocking should also be considered. The effect of different neutron and proton distributions would also play an important role in determining the asymmetry dependence as discussed by Shen *et al.*[6] Any further refinement will destroy the simple feature of our analytic expression (21), however, it may be necessary to incorporate these details as the heavy-ion reaction cross sections have a potential of determinating the surface texture of nuclear densities.

[1]P. J. Karol, Phys. Rev. C **11**, 1203 (1975).
[2]R. Bass, *Nuclear reactions with heavy ions: Texts and Monographs in Physics* (Springer-Verlag, Berlin, 1980).
[3]S. K. Gupta and S. Kailas, Z. Phys. A **317**, 75 (1984).
[4]A. Vitturi and F. Zardi, Phys. Rev. C **36**, 1404 (1987).
[5]R. M. Devries and J. C. Peng, Phys. Rev. C **22**, 1055 (1980).
[6]W. Shen, B. Wang, J. Feng, W. Zhan, Y. Zhu, and E. Feng, Nucl. Phys. **A491**, 130 (1989).
[7]S. Kox, A. Gamp, C. Perrin, J. Arvieux, R. Bertholet, J. F. Bruandet, M. Buenerd, R. Cherkaoui, A. J. Cole, Y. El Masri,

N. Longequeue, J. Menet, F. Merchez, and J. B. Viano, Phys. Rev. C **35**, 1678 (1987).
[8]C. Perrin, S. Kox, N. Longequeue, B. J. Viano, M. Buenerd, R. Cherkaoui, A. J. Cole, A. Gamp, J. Menet, R. Ost, R. Bertholet, C. Guet, and J. Pinston, Phys. Rev. Lett. **49**, 1905 (1982).
[9]M. E. Brandan, J. Phys. G **9**, 197 (1983).
[10]S. Kox, A. Gamp, R. Cherkaoui, A. J. Cole, N. Longequeue, J. Menet, C. Perrin, and J. B. Viano, Nucl. Phys. **A420**, 162 (1984).
[11]M. Buenerd, A. Lounis, J. Chauvin, D. Lebrun, P. Martin, G. Duhamel, J. C. Gondrand, and P. de Saintgnon, Nucl. Phys. **A424**, 313 (1984).
[12]N. Alamos, F. Auger, J. Barrette, B. Berthier, B. Fernandez, J. Gastebois, and L. Papineau, Phys. Lett. **137B**, 37 (1984).
[13]F. Bruandet, J. Phys. (Paris) Colloq. **47**, C4-125 (1986).
[14]J. Jaros, A. Wagner, L. Anderson, O. Chamberlain, R. Z. Fuzesy, J. Gallup, W. Gorn, L. Schroeder, S. Shannon, G. Schapiro, and H. Stiner, Phys. Rev. C **18**, 2273 (1978).
[15]A. J. Cole, W. D. Rae, M. E. Branden, A. Dacal, B. G. Harvey, R. Legrain, M. J. Murphy, and R. G. Stokstad, Phys. Rev. Lett. **47**, 1705 (1981).
[16]M. Buenerd, J. Pinston, A. J. Cole, C. Guet, D. Lebrun, J. M. Loiseaux, P. Martin, E. Monnard, J. Mougey, H. Nifenecker, R. Ost, P. Perrin, C. Ristori, P. DeSaintignon, F. Schussler, L. Carlen, H. A. Gustafsson, B. Jakobsson, T. Johansson, J. Jonsson, J. Krumlinde, I. Otterlund, H. Ryde, B. Schröder, G. Tibell, J. P. Bondrof, and O. B. Nilesen, Phys. Lett. **102B**, 242 (1981).
[17]H. G. Bohlen, M. R. Clover, G. Ingold, H. Lettau, and W. Von Oertzen, Z. Phys. A **308**, 121 (1982).
[18]W. Treu, N. Frohlich, W. Galster, P. Duck, and H. Voit, Phys. Rev. C **22**, 2462 (1980).
[19]L. W. Townsend and J. W. Wilson, Rad. Res. **106**, 283 (1986).
[20]J. Friedrich, N. Voegler, Nucl. Phys. A **373**, 192 (1982).
[21]G. Giacomelli, *Total Cross Section Measurements: Progress in Nuclear Physics* (Pergamon, New York, 1970), Vol. 12.
[22]S. K. Charagi, S. K. Gupta, and S. Kailas, Pramana (to be published).
[23]H. A. Enge, *Introduction to Nuclear Physics* (Addison-Wesley, Reading, Mass., 1966).
[24]W. V. Schröder and J. R. Huizenga, Annu. Rev. Nucl. Sci. **27**, 465 (1977).
[25]G. R. Satchler and W. G. Love, Phys. Rep. **55C**, 183 (1979).
[26]S. E. Vigdor, D. G. Kovar, P. Sperr, J. Mahoney, A. Menchaca Rocha, C. Olmer, and M. S. Zisman, Phys. Rev. C **20**, 2147 (1979).
[27]I. Angeli, M. Csatlos, Atomki. Kozlemenyek. **20**, 1 (1978).
[28]L. W. Townsend and J. W. Wilson, NASA Ref. Pub. **1134** (1985).